Peng *et al. BMC Plant Biology* (2025) 25:1315
https://doi.org/10.1186/s12870-025-07408-7

BMC Plant Biology

RESEARCH Open Access

Reconstructing the evolutionary trajectory of *Chamaelirium* (Melanthiaceae) through phylogenomics: insights from plastome dynamics and historical biogeography

Jing-Yi Peng[1†], Xian-Han Huang[1†], Xin-Jian Zhang[1], Joonhyung Jung[2], Changkyun Kim[3], Tae-Hee Kim[4], Noriyuki Tanaka[5], Shiou Yih Lee[6], Joo-Hwan Kim[7*], Hang Sun[1*] and Tao Deng[1*]

Abstract

Background The East Asia-eastern North America disjunction represents a classic biogeographic pattern, widely interpreted as a relic of Tertiary temperate forests that were widespread across the Northern Hemisphere. Although this pattern has been well-documented in woody plants, disjunctions in herbaceous taxa have remained relatively unexplored, despite their potential to provide significant evolutionary insights. The genus *Chamaelirium* represents a suitable system for investigating herbaceous discontinuity between East Asia and eastern North America. However, unresolved section-level relationships within the genus based on limited molecular data indicated that its systematics still required clarification. Here, we generated complete plastid genomes (plastomes) for five *Chamaelirium* species covering all sections of the genus and performed the phylogenomic analysis for the first time with a reexamination of its historical biogeography.

Results Comparative genomic analyses revealed that *Chamaelirium* plastomes exhibit relatively conserved structures and content organization; however, several noteworthy variations were observed. Specifically, an expansion of the IR region was identified in the plastid genomes of *C. viridiflorum* and *C. chinense*, while the loss of the *rps*16 gene in *C. japonicum* and *C. koidzumianum* may have contributed to a reduction in genome size. Phylogenetic analysis combined with niche modeling revealed two major clades within *Chamaelirium*, corresponding to the two sections proposed in traditional classifications. Robust support for interspecific relationships within each section was provided by morphological characters, plastome variations, and geographical distributions. Divergence time estimates and ancestral region reconstructions indicate that *Chamaelirium* originated in the Eocene (ca. 53.03 Ma), with the ancestral

[†]Jing-Yi Peng and Xian-Han Huang contributed equally to this work.

*Correspondence:
Joo-Hwan Kim
kimjh2009@gachon.ac.kr
Hang Sun
sunhang@mail.kib.ac.cn
Tao Deng
dengtao@mail.kib.ac.cn

Full list of author information is available at the end of the article

© The Author(s) 2025. **Open Access** This article is licensed under a Creative Commons Attribution-NonCommercial-NoDerivatives 4.0 International License, which permits any non-commercial use, sharing, distribution and reproduction in any medium or format, as long as you give appropriate credit to the original author(s) and the source, provide a link to the Creative Commons licence, and indicate if you modified the licensed material. You do not have permission under this licence to share adapted material derived from this article or parts of it. The images or other third party material in this article are included in the article's Creative Commons licence, unless indicated otherwise in a credit line to the material. If material is not included in the article's Creative Commons licence and your intended use is not permitted by statutory regulation or exceeds the permitted use, you will need to obtain permission directly from the copyright holder. To view a copy of this licence, visit http://creativecommons.org/licenses/by-nc-nd/4.0/.

area of its crown most likely located in East Asia. The divergence between the East Asian and North American lineages occurred during the early Miocene (ca. 17.95 Ma), with the Bering Land Bridge acting as a corridor; subsequent global cooling likely facilitated the establishment of an intercontinental disjunction in the genus. The rise of the East Asian monsoon during the late Miocene may have further triggered its diversification in East Asia.

Conclusions Our phylogenomic analyses of *Chamaelirium* have resolved previously ambiguous section-level relationships and provide novel genomic resources for clarifying infrageneric boundaries. Furthermore, by presenting *Chamaelirium* as a new case, this study highlights the significance of the Miocene and the Bering Land Bridge in shaping the East Asian-North American disjunction pattern among herbaceous plants.

Keywords Chamaelirium, Phylogenomics, Niche modeling, Miocene, Bering land bridge, East Asian monsoon

Background

Disjunct distribution, a biogeographic pattern characterized by discontinuous distributions of organisms, represents a critical focus for understanding global biodiversity patterns and evolutionary histories [1–3]. As one of the most prominent disjunctions, the intercontinental disjunction between eastern North America and East Asia has long attracted considerable attention from many researchers [4–6]. This disjunction is generally explained as a relic of the temperate forests across the Northern Hemisphere during the Tertiary [6, 7]. Climatic and orogenic changes have caused this fragmentation, including global cooling that drove glaciations in Europe and other regions with higher northern latitudes during the Neogene and the Quaternary, and Neogene orogenies as well as subsequent development of the xeric and high-elevation coniferous floras in western North America and western East Asia [5, 8]. Both the Bering and North Atlantic land bridges are considered to have facilitated the development of deciduous forests during the Tertiary and to have served as important corridors for floristic exchanges between eastern North America and East Asia [6, 8, 9]. Some studies suggest that cases of migration out of Asia or North America via both land bridges are supported among examined discontinuous lineages, though migration patterns from Asia to North America via the Bering Land Bridge predominate [5, 8]. However, despite the East Asia-eastern North America disjunction pattern being the result of multiple complex processes, most discontinuous taxa are represented by woody plants, while herbaceous lineages account for only a small proportion [5, 6, 10]. Consequently, relatively few studies have explored the evolution of this disjunction in herbaceous groups.

Chamaelirium Willd. (Melanthiaceae) (Fig. 1) provides a promising case for advancing studies on herbaceous disjunction patterns between eastern North America and East Asia. Historically considered monotypic, *Chamaelirium* underwent a taxonomic revision in 2017 when Tanaka [11] merged the genus *Chionographis* Maxim. into *Chamaelirium*. This reclassification, based on morphology (e.g., flower structure, tepal characteristics, and sexual system), chromosome counts, and phenology, divided the genus into two sections: sect. *Chamaelirium* and sect. *Chionographis* [11, 12]. The former section is represented solely by *C. luteum* (L.) A.Gray, found in eastern North America, and the latter was further subdivided into two subsections, with distributions in East Asia (China, Korea, Japan, Laos, and Vietnam). The subsect. *Chionographis* includes four species: *C. koidzumianum* (Ohwi) N.Tanaka, *C. cordifolium* (N.Tanaka) N.Tanaka, *C. hisauchianum* (Okuyama) N.Tanaka, and *C. japonicum* (Willd.) N.Tanaka; and another subsect. *Cathayana* encompasses *C. actinomorphum* (Aver. & N.Tanaka) N.Tanaka & Aver., *C. chinense* (K.Krause) N.Tanaka, *C. shiwandashanense* (Y.Feng Huang & R.H.Jiang) N.Tanaka, and *C. nanlingense* (L.Wu, Y.Tong & Q.R.Liu) N.Tanaka. Since 2017, recent taxonomic work has further expanded the genus to 12 formally recognized species through descriptions of three Chinese endemics, i.e., *C. viridiflorum* L.Wang, Z.C.Liu & W.B.Liao [13], *C. shimentaiense* Y.H.Tong, C.M.He & Y.Q.Li [14], and *C. jiuwanshanense* Ying Qin & Yan Liu [15].

Despite morphological and phenological coherence within Tanaka's taxonomic framework of *Chamaelirium*, molecular validation of infrageneric relationships remains necessary, including for species described after 2017, whose evolutionary relationships remain unresolved at the molecular level. Kim et al. [16] previously conducted a biogeographic study of Melanthiaceae using four plastid markers (*atp*B, *rbc*L, *mat*K, and *ndh*F) involving four *Chamaelirium* species, suggesting that the North American lineage of *Chamaelirium* may follow the "out-of-North America" origin pattern. However, they were unable to recover the subsect. *Chionographis* as monophyletic in phylogenetic analysis, as *C. japonicum* (subsect. *Chionographis*) clustered with *C. chinense* (subsect. *Cathayana*). This discordance highlights the need for additional molecular data with informative loci to reassess the pending genetic relationship within *Chamaelirium* and potentially the biogeography of the genus.

The plastid genome (plastome), due to its high gene density, conserved nature, and moderate evolution rate,

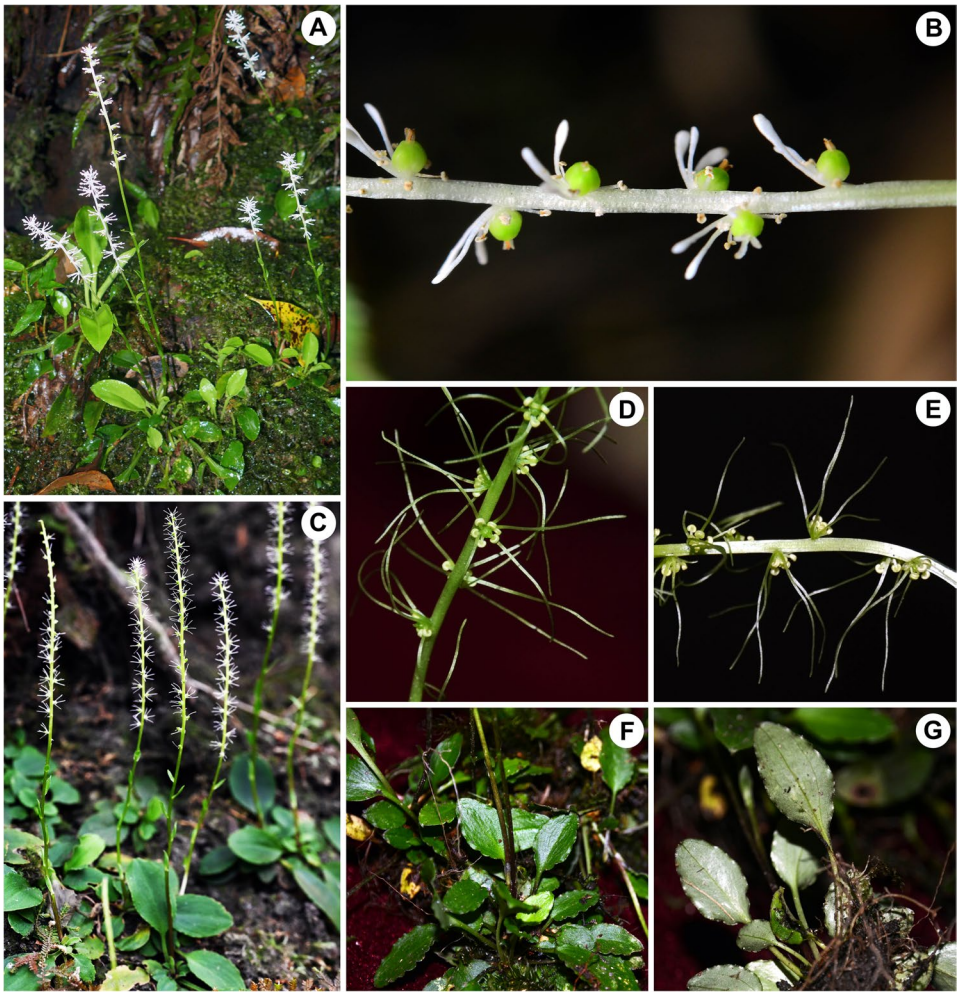

Fig. 1 Photos of three *Chamaelirium* species. **A-B** *C. chinense* and its female flowers (photographed by Xin-jian Zhang and Cheng Zhang respectively). **C** *C. shimentaiense* (photographed by Li Li). **D-G** Male flowers and leaves of *C. viridiflorum* (photographed by Wan-yi Zhao). All photos used have been approved by the photographers

is considered a valuable tool for resolving systematic relationships at different taxonomic levels in plants, whereas mutational events such as substitution, translocation, insertion, and deletion within the genome often provide important clues for studying large-scale evolutionary processes [17–20]. However, genomic resources for *Chamaelirium* are critically limited to date, with only the *C. japonicum* plastome reported by Bodin et al. [21], accompanied by comparative analyses with related taxa. Consequently, we have newly sequenced and assembled the plastid genomes of five *Chamaelirium* species (*C. chinense*, *C. japonicum*, *C. viridiflorum*, *C. koidzumianum*, and *C. luteum*) in this study, which cover the two recognized sections of the genus. Several research objectives were clearly defined: (i) to investigate plastome dynamics within *Chamaelirium*, (ii) to reconstruct its phylogenetic relationships, and (iii) to reassess the biogeographic events associated with the formation of the East Asian-eastern North American disjunction for this genus.

Results

Comparative genomics within Chamaelirium

We successfully assembled complete circular plastid genomes of five *Chamaelirium* species, all exhibiting the typical quadripartite structure (Fig. 2A). These genomes comprised a pair of inverted repeat (IR) regions (27,398–27,541 bp) separated by a large single-copy (LSC) region (81,654–84,329 bp) and a small single-copy (SSC) region (18,206–18,244 bp), with total genome sizes ranging from 154,657 bp to 157,655 bp. All plastomes included 8 rRNA and 38 tRNA genes, but the number of protein-coding gene (CDS) varied among species. *C. chinense*, *C. viridiflorum*, and *C. luteum* encoded 89 CDS, while *C. japonicum* and *C. koidzumianum* possessed 88 CDS due to the loss of the *rps*16 gene. The overall GC content ranged from 37.7% to 38.0%, with corresponding values of 35.9%–36.0% in the LSC, 31.2%–31.4% in the SSC, and 42.4%–42.5% in the IR regions. Twenty-one genes were duplicated in the IR regions, and 18 intron-containing

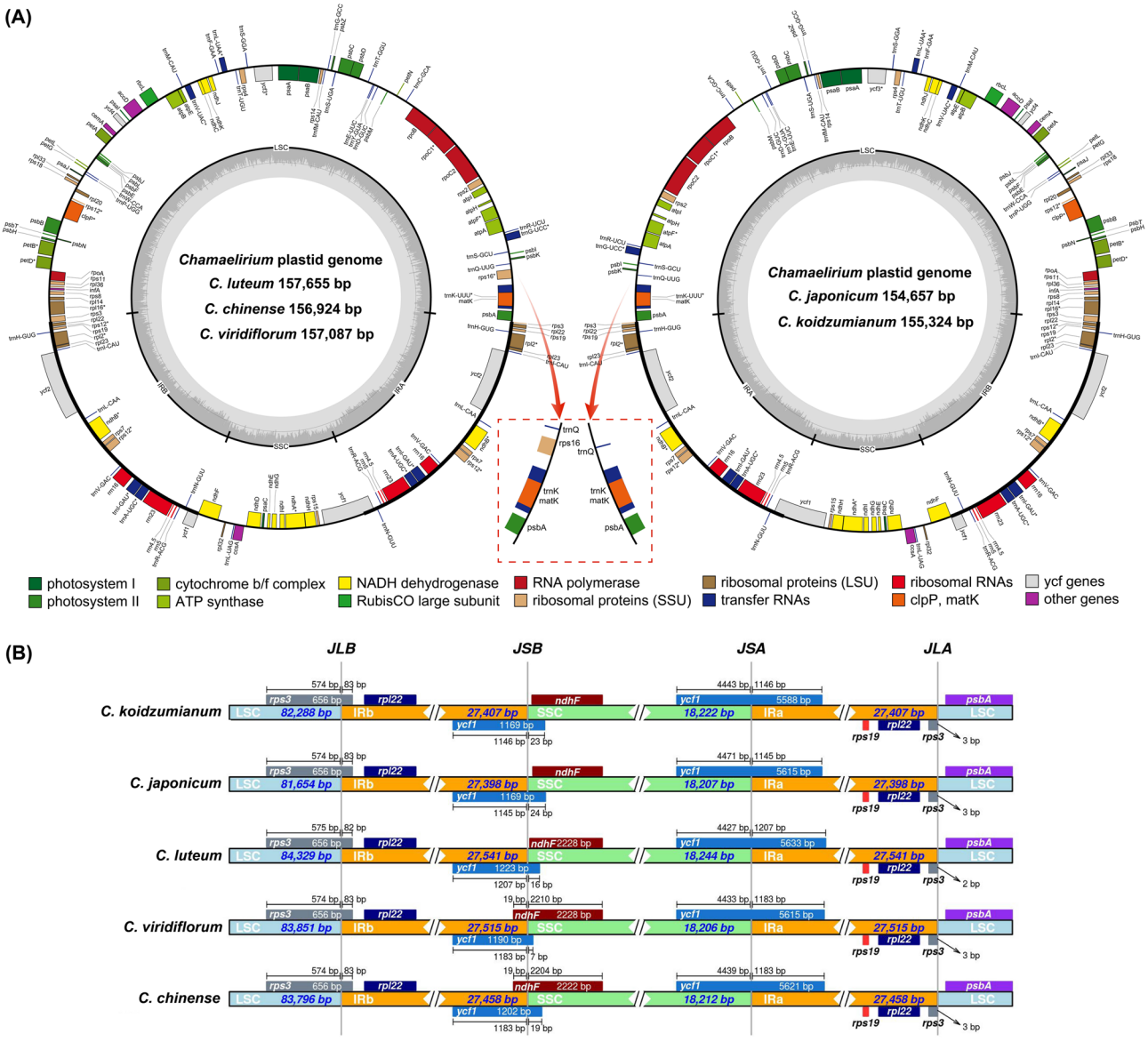

Fig. 2 Plastome basic characters of *Chamaelirium* species. **A** Gene map of *Chamaelirium* plastomes, with genome sizes ranging from 154,657 bp to 157,655 bp; the *rps*16 gene is absent in *C. japonicum* and *C. koidzumianum*. Genes are color-coded by function, with genes inside and outside of the circle transcribed in clockwise and counterclockwise directions, respectively. The darker gray area in the inner circle corresponds to GC content, whereas the lighter gray corresponds to AT content. **B** Plastome boundaries (LSC/IRb, IRb/SSC, SSC/IRa, IRa/LSC) in *Chamaelirium*

genes were identified, with *clp*P and *ycf*3 each harboring two introns (Table 1 and S1). Visualization of the plastid genome boundaries of the five *Chamaelirium* species found six genes (*rps*3, *rpl*22, *ycf*1, *ndh*F, *rps*19, and *psb*A) near the four junctions (LSC/IRb, IRb/SSC, SSC/IRa, and IRa/LSC) (Fig. 2B). Of these, *ycf*1 and *rps*3 spanned across the boundary, forming pseudogenes (ψ*ycf*1 and ψ*rps*3) at the IRb/SSC boundary and within the IRa region, respectively. Additionally, the *ndh*F gene extended 19 bp into the IRb in *C. chinense* and *C. viridiflorum* but was fully contained within the SSC region in *C. japonicum*, *C. koidzumianum*, and *C. luteum*.

Adaptive evolutionary analysis was performed using shared CDS from the five *Chamaelirium* species, and we averaged the Ka/Ks values for each gene as their respective final Ka/Ks (Ka/Ks: the ratio of non-synonymous to synonymous nucleotide substitution rates). The Ka/Ks > 1 and < 1 indicated that the gene was under positive selection and purifying selection, respectively. Our analysis revealed that nearly all of the genes were undergoing strong purifying selection in the *Chamaelirium* plastid genome, with the exception of *ycf*2, which was subjected to positive selection (Fig. S1). Notably, 13 genes without any synonymous changes (Ks = 0), including *rps*19, *rps*15, *rpl*36, *rpl*33, *rpl*23, *rpl*2, *psb*M, *psb*J, *psb*I, *psb*F, *pet*L,

Table 1 Basic information on the five newly assembled plastomes of *Chamaelirium* species

Species	Size (bp)				Gene number					GC content (%)				GenBank accession
	Total	LSC	SSC	IR	Total	CDS	tRNA	rRNA		Total	LSC	SSC	IR	
Chamaelirium chinense	156,924	83,796	18,212	27,458	135	89	38	8		38.0%	36.0%	31.2%	42.5%	PV786079
Chamaelirium viridiflorum	157,087	83,851	18,206	27,515	135	89	38	8		37.7%	35.9%	31.2%	42.4%	PV786080
Chamaelirium luteum	157,655	84,329	18,244	27,541	135	89	38	8		37.7%	36.0%	31.3%	42.4%	PV786081
Chamaelirium japonicum	154,657	81,654	18,207	27,398	134	88	38	8		37.8%	36.0%	31.4%	42.5%	PV786082
Chamaelirium koidzumianum	155,324	82,288	18,222	27,407	134	88	38	8		37.7%	36.0%	31.3%	42.5%	PV786083

To facilitate the efficient retrieval of all sequences for existing species in the NCBI database, synonymous names were used during the registration of some newly sequenced species. The accession numbers PV786079, PV786082, and PV786083 correspond to *Chionographis chinensis*, *Chionographis japonica*, and *Chionographis koidzumiana* in the NCBI database, respectively

*pet*G, and *ndh*G, yielded an indeterminate Ka/Ks value. Nucleotide diversity (Pi) analysis detected highly variable hotspots in the plastid genome (Fig. S2). Pi values for intergenic regions (IGS) ranged from 0 to 0.07, while gene regions (GS) ranged from 0 to 0.01389. We defined IGS with Pi > 0.05 and GS with Pi > 0.0125 as hotspots. Three highly variable IGS (*psb*T–*psb*N, *trn*S-GCU–*trn*G-UCC, and *rps*3–*psb*A) and three GS (*trn*T-GGU, *rpl*20, and *ndh*F) were identified, with Pi values of 0.07, 0.06757, 0.06582, 0.01389, 0.01356, and 0.01327, respectively.

Phylogenetic reconstruction and niche modeling for *Chamaelirium*

Alignments of 82 shared CDS produced a phylogenetic matrix of 82,251 bp, encompassing 19 samples from 18 species. Phylogenetic analysis using maximum likelihood (ML) and Bayesian inference (BI) yielded consistent and well-resolved topologies (Fig. 3). *Chamaelirium* was strongly supported as a monophyletic group (BP = 1, BS = 100) and was sister to a clade comprising *Heloniopsis* A. Gray and *Ypsilandra* Franch. Two major clades were identified within *Chamaelirium*, with genomic and morphological characters mapped onto the phylogenetic tree to trace patterns of variation across clades. The most basal clade, represented solely by *C. luteum* from the sect. *Chamaelirium*, established a sister relationship to the remaining species (BP = 1, BS = 100). Another clade (BP = 1, BS = 100), corresponding to the sect. *Chionographis*, encompassed two subclades: one formed by *C. viridiflorum* and *C. chinense* from the subsect. *Cathayana* (BP = 1, BS = 100); and the other comprising *C. japonicum* and *C. koidzumianum* from the subsect. *Chionographis* (BP = 1, BS = 100).

Ecological niche modeling evaluated the area under the curve (AUC) values averaged over all 10 replicate runs exceeded 0.95 for all three Sect. (0.979 for *Chamaelirium*, 0.998 for *Cathayana*, and 0.994 for *Chionographis*), indicating high predictive reliability of the modeling. The modeling (Fig. 4C) showed that the predicted distribution of the sect. *Chamaelirium* closely matched actual occurrence records in eastern North America. In contrast, the actual and predicted potential distributions of the subsect. *Cathayana* and subsect. *Chionographis* were confined to East Asia. Specifically, suitable habitats for the subsect. *Cathayana* were predicted to expand from southeastern China into coastal regions of Vietnam and southern Japan, while those for the subsect. *Chionographis* were predicted to extend beyond their current range in Japan and Korea into southeastern China.

Molecular dating and ancestral region reconstruction for *Chamaelirium*

The BEAST analysis (Fig. 4A) indicated that *Chamaelirium* diverged from its nearest sister group during

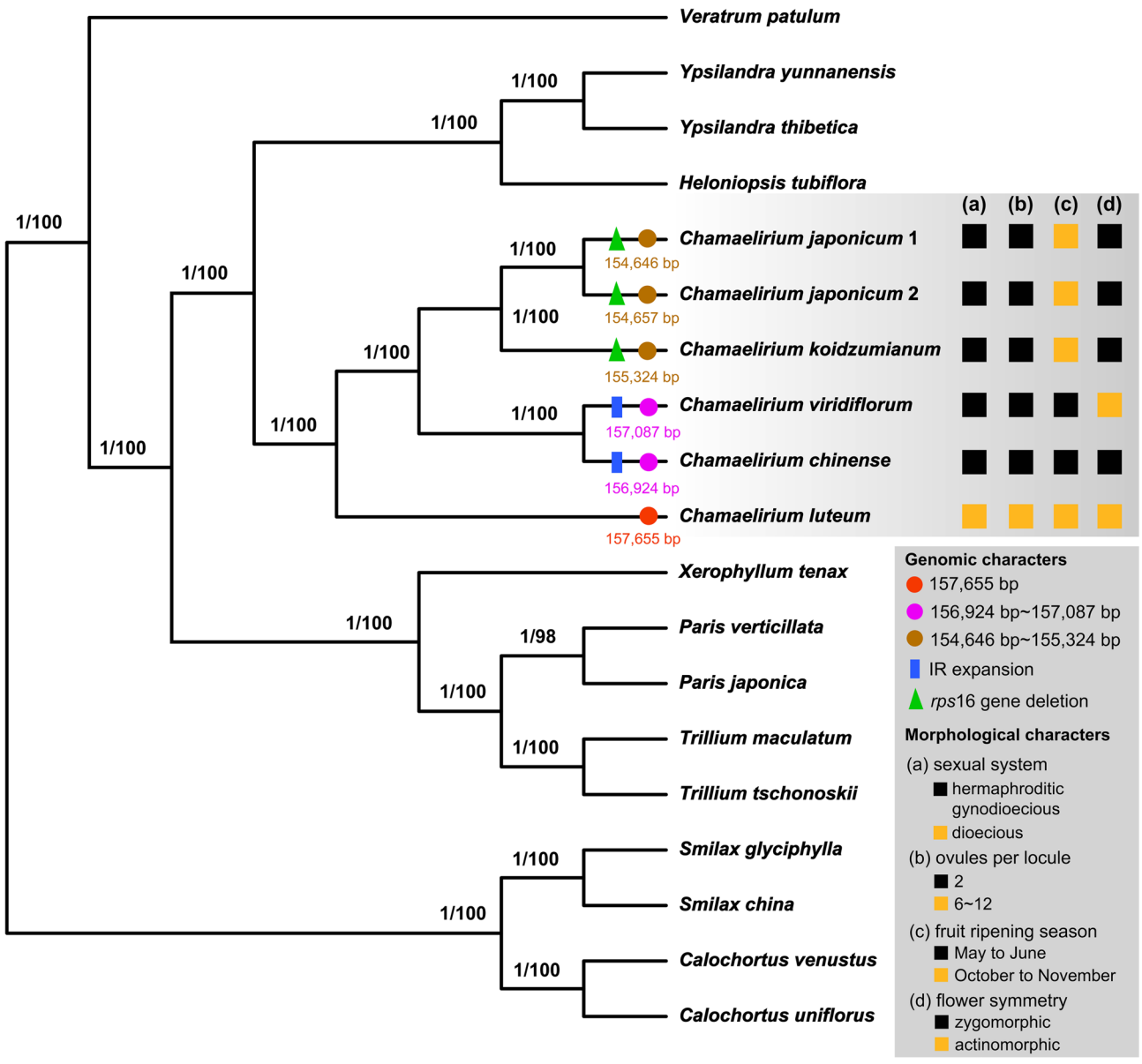

Fig. 3 Phylogeny, genomic and morphological characters of *Chamaelirium*. Phylogeny was inferred based on 82 shared protein-coding genes (CDS), and numbers at the nodes indicate the Bayesian posterior probabilities (BP) (left) and ML bootstrap supports (BS) (right). Genomic and morphological variations within *Chamaelirium* were mapped onto a phylogenetic tree

the Eocene at ca. 53.03 Ma (Node 1, 95% HPD: 70.72–32.33 Ma). Within this genus, the divergence between the North American clade (sect. *Chamaelirium*) and the East Asian clade (sect. *Chionographis*) occurred around 17.95 Ma (Node 2, 95% HPD: 34.82–6.67 Ma) during the Miocene. The split of the crown of the East Asian clade commenced at ca. 8.13 Ma (Node 3, 95% HPD: 17.55–2.61 Ma). Based on the pruned dated tree, the BBM method estimated that the ancestral region of the crown of *Chamaelirium* was ambiguous, with a slightly higher probability in East Asia (49%) than in North America (44%) (Fig. 4B).

Discussion

Plastome dynamics for *Chamaelirium*

The present study provides five newly plastid genomes from *Chamaelirium* and reveals several striking differences that may reflect evolutionary events. Typically, changes in plastome size result from IR contraction or expansion, gene loss or duplication [22–24]. Notably, we observed *rps*16 gene loss in *C. japonicum* and *C. koidzumianum*, although it was retained in the other three species (Fig. 2A). Bodin et al. [21] also reported the deletion of this gene in their *C. japonicum* sample. At least 17 genes, including the *rps*16, were commonly lost in angiosperms [25]. We hypothesize that the absence of

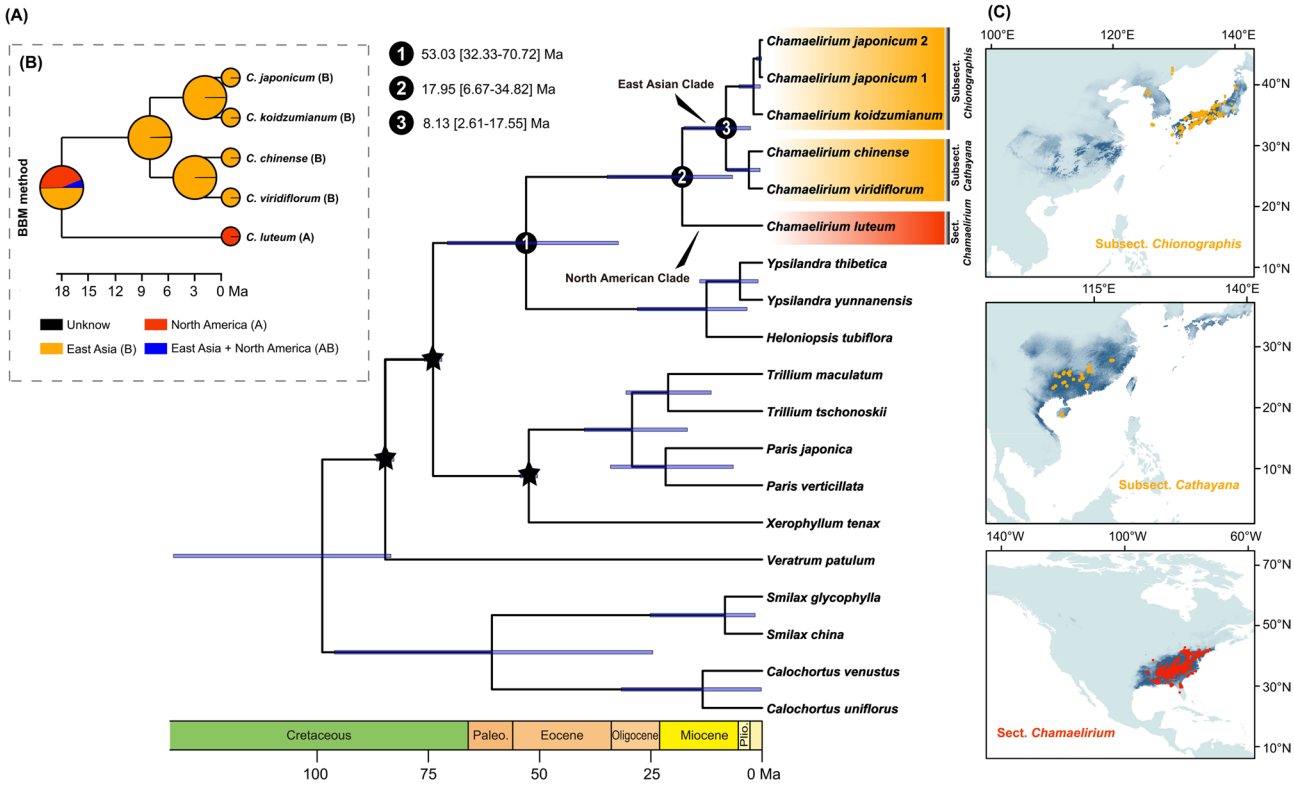

Fig. 4 Divergence time estimation and biogeographical reconstruction of *Chamaelirium*. **A** Chronogram of *Chamaelirium* derived from the MCC tree based on BEAST analysis. Section names are overlaid with red and yellow shading to denote their distributions in North America and East Asia, respectively. The blue bars represent the highest posterior density (HPD) intervals of the divergent age (HPD = 95%), and the stars show calibration points for the molecular dating. Circles with numbers indicate key nodes (nodes 1–3), giving mean age and HPD intervals. **B** Ancestral region reconstruction of *Chamaelirium* using Bayesian binary method (BBM). The distribution of *Chamaelirium* species is divided into two regions: (A) North America and (B) East Asia; the different colors in the pie charts display the relative probabilities for each distribution area being inferred. **C** Maps showed occurrence points for species within each section, with shades corresponding to the possible distribution predicted by MaxEnt v.3.4

the *rps*16 gene may contribute to the smaller plastome sizes of *C. japonicum* (154,657 bp) and *C. koidzumianum* (155,324 bp) compared to the other three species (156,924–157,655 bp), but whether this gene has been transferred to their nuclear genome requires further investigation [21, 26]. Visualization of IR boundary junctions revealed significant IR expansion in *C. viridiflorum* and *C. chinense*, allowing the *ndh*F gene to cross the IRb/SSC boundary (Fig. 2B). Despite such expansions, *C. luteum* still retained the largest plastome (157,655 bp), suggesting that IR expansion may not be the primary factor driving genome size enlargement in *Chamaelirium*.

Adaptive evolution of plastid genomes in response to environmental pressures is a common phenomenon, as the environment can exert strong selective forces on plant evolution [27]. The ratio of non-synonymous to synonymous nucleotide substitution rates (Ka/Ks) serves as a key measure of selective pressure on genes [28]. In our analysis, positive selection was detected only for the *ycf*2 gene in *Chamaelirium* plastomes (Fig. S2). This gene encodes products essential for chloroplast protein input and cell survival [17, 29], and the detection of positive selection acting on *ycf*2 further highlights its potential adaptive role in the evolutionary process of *Chamaelirium*. While most genes were under strong purifying selection, a prevalent mechanism in natural selection that continuously eliminated harmful mutations [30], purifying selection on these plastid genes in *Chamaelirium* would be the evolutionary result of the retention of the adaptive characters of species. Mutational events did not occur randomly but were concentrated in hotspot regions of the plastid genome [31, 32]. The identification of highly informative and variable genomic regions is crucial for plant phylogenetic reconstruction and for advancing DNA barcoding development [33]. We further proposed six variable hotspot regions in this study, localized in *psb*T–*psb*N, *trn*S-GCU–*trn*G-UCC, *rps*3–*psb*A, *trn*T-GGU, *rpl*20, and *ndh*F (Fig. S2). Taking into account the cost and time constraints associated with plastome sequencing, hotspot regions could provide an ideal compromise between the expense of ultra-barcodes (such as the whole plastid genome) and the issue of limited genetic variation for standard barcodes [34]. As potential candidates, these regions are expected to be

developed into novel DNA markers in the future, which will contribute to expanding the datasets of taxon-specific barcoding and be applied to phylogenetic inference and species identification in *Chamaelirium*.

Resolving *Chamaelirium* phylogeny from multiple perspectives

Our phylogenetic results based on plastid genomic data support the monophyly of *Chamaelirium*, with two major clades corresponding to the North American sect. *Chamaelirium* and the East Asian sect. *Chionographis*, consistent with the findings of Kim et al. [16] (Fig. 3). Tanaka [11, 12] proposed that these two sections differ markedly in several morphological aspects: the former is dioecious (vs. hermaphroditic or gynodioecious in the latter) and possesses ovaries with 6–12 ovules per locule (vs. with only two), suggesting that each section can be strikingly defined as monophyletic. Within the sect. *Chionographis*, following the infrageneric taxonomic framework by Tanaka [11], the newly described species *C. viridiflorum* (published in 2018) should be assigned to the subsect. *Cathayana* [13], a placement now confirmed by our molecular data for the first time. Notably, our results also resolved long-standing conflicts arising from the use of limited molecular markers [16], providing strong support for the monophyly of the subsect. *Chionographis* as sister to the subsect. *Cathayana*, with the two subsections distinguishable by floral symmetry (zygomorphic vs. actinomorphic; only *C. chinense* exhibits zygomorphic flowers in the subsect. *Cathayana*) and fruit ripening season [11, 13]. Meanwhile, plastid genome variations further reflected infrageneric genetic relationships, including changes in plastome size (sect. *Chamaelirium* > subsect. *Cathayana* > subsect. *Chionographis*), IR region expansion (subsect. *Cathayana*), and the deletion of the *rps*16 gene (subsect. *Chionographis*), thereby providing additional evidence for phylogenetic divergence within *Chamaelirium*.

From the perspective of geographical evidence (Fig. 4C), significant differences were observed in the distributions of each *Chamaelirium* section: the sect. *Chamaelirium* is restricted to eastern North America, as are the subsect. *Cathayana* to southeastern China and the subsect. *Chionographis* to the Korea-Japan region, respectively. Our ecological niche modeling further supported these findings, indicating that the sect. *Chamaelirium* and the sect. *Chionographis* separately occupy distinct suitable habitats in North America and East Asia. The results integrating geographical distribution and niche modeling revealed a clear spatial segregation along phylogenetic lineages, which may imply the presence of phylogenetic conservatism in the distribution of each section. This integrative approach, combining phylogeny and niche modeling to elucidate evolutionary relationships has also been applied in several other taxa, such as *Uncaria* (Rubiaceae Juss.) [35] and *Trinomia* (Halictidae) [36]. However, despite our modeling identifying extensive suitable habitats for East Asian taxa across space, discrepancies with their actual distributions remained. Potential biases in modeling projections could not be entirely ruled out (e.g., geographical extrapolation) [37]; a widely accepted explanation is that geographic barriers, biotic interactions, or other barriers to gene flow may prevent species from colonizing all potentially suitable habitats [36].

Historical biogeography inference

Our molecular dating estimated the stem age of *Chamaelirium* at ca. 53.03 Ma (Fig. 4A), aligning closely with previous estimates of Kim et al. [16] (ca. 55.8 Ma) and Yang et al. [38] (ca. 49.76 Ma). However, our biogeographic reconstruction for the crown ancestor of *Chamaelirium* contrasts with the conclusion of Kim et al. [16] that the North American lineage originated via in situ evolution. Instead, we propose that East Asia is the more likely ancestral area for the North American lineage of *Chamaelirium*, though our BBM analysis provided only weak support for this hypothesis, with marginally higher probabilities for East Asia (Fig. 4B). This result may be influenced by our expanded taxon sampling and the use of different datasets without outgroups. Our conclusion is also further corroborated by morphological evidence: Tanaka [11] considered the North American sect. *Chamaelirium* to be more advanced than the East Asian sect. *Chionographis* in its sexual characters since its dioecy as an apomorphy was likely to be derived from the gynodioecy and hermaphroditism of the latter. This inference parallels the ancestral region assessment for the genus *Sageretia* Brongn. (without outgroups) based on morphology [39].

Plant interchanges between Eurasia and North America are thought to have occurred via the North Atlantic Land Bridge (NALB) and the Bering Land Bridge (BLB), two major migration routes that facilitated the dispersal of taxa in the Northern Hemisphere at different times [4, 5, 9]. The NALB began to gradually disintegrate from the Eocene to Miocene (ca. 50–15 Ma), although intermittent island chains may have allowed limited interchanges [7, 9, 40, 41]. As a critical spread pathway for thermophilic taxa [5], the NALB became less favorable for warm-climate taxa since the early Oligocene [42]. In contrast, the BLB, active from at least the early Paleocene to its closure between 7.4 and 4.8 Ma, functioned as an important corridor for temperate taxa [5, 7]. Combined with our inferred crown age for *Chamaelirium*, the separation of the North American and East Asian lineages can be traced back to ca. 17.95 Ma (Fig. 4A). This timing is slightly younger than that proposed by Kim et al. [16]

(ca. 23.5 Ma), a gap that may stem from the use of distinct calibration points applied in our expanded dataset. Therefore, the BLB appears to have been the more likely route for *Chamaelirium* disjunction, a hypothesis further supported by multiple studies reporting that the vast majority of herbaceous lineages occurring disjunction during the Miocene likewise utilized the BLB for migration between East Asia and North America [5, 10, 43, 44]. The peak warming phase of the late Middle Miocene Climatic Optimum (MMCO, ca. 17–15 Ma) [45] may have enabled the migration of *Chamaelirium* from East Asia to the high latitudes of the Northern Hemisphere to reach North America through the BLB, followed by southward retreat during subsequent cooling. Continued global cooling during the late Miocene likely interrupted further interchanges between the East Asian and North American lineages, ultimately establishing their intercontinental disjunction. Similar migration patterns and formation mechanisms have also been observed in the intercontinental disjunction of several examined herbaceous lineages, such as the *Amianthium* A. Gray-*Veratrum* L. clade in Melanthiaceae [16] and *Apios* Fabr. (Fabaceae) [46]. Notably, organisms crossing the BLB must be able to survive the cold and dark winters in the high-latitude Bering region [42], while certain inherent morphological characters of plants may have played crucial roles in this process, as exemplified by the hooked persistent upper calyx lobes on *Phryma* fruits [43]. For *Chamaelirium*, its tubers surviving the winter may confer an adaptive advantage in this regard [11], as has been reported in *Apios*, which shares a similar character [46]. Additionally, the rise and development of the Asian monsoon climate increased humidity in previously arid regions of East Asia since the Miocene [47–49], promoting the dispersal and divergence of sections *Thibeticae*, *Axiparis*, and *Euthyra* in *Paris* L. within Melanthiaceae [50], and may also have created favorable conditions for the spread of *Chamaelirium*. The crown divergence of the East Asian clade of *Chamaelirium* occurred at ca. 8.13 Ma, aligning temporally with the establishment of the Indian and East Asian monsoons (ca. 9–8 Ma) [51]. Under this scenario, the presence of winged seeds in *Chamaelirium* [11] suggests a potential adaptation to anemochory, which may have further driven its dispersal and subsequent diversification throughout East Asia.

Conclusion

In this study, we conducted the first plastid phylogenomics analyses for *Chamaelirium* using expanded datasets and taxon sampling, coupled with a review of its historical biogeography. Our results not only clarified the phylogenetic position of *C. viridiflorum* (a new species published in 2018) for the first time but also robustly addressed previous phylogenetic uncertainties, providing strong support for the current taxonomic framework of the genus. Besides, the biogeographic inferences indicate that the Bering Land Bridge and global cooling likely played pivotal roles in shaping the East Asian-North American disjunction of *Chamaelirium*, while the establishment and strengthening of the East Asian monsoon may have significantly influenced the subsequent diversification of this genus in East Asia. For future research directions, further increasing sampling density will be essential. In addition to consolidating the phylogeny and clarifying finer-scale biogeographic patterns, investigating the adaptive evolution of morphological characters also will be crucial for advancing our understanding of this genus.

Materials and methods

Plant materials, DNA extraction, and sequencing

According to the latest taxonomic revision of *Chamaelirium* and incorporating recently described new taxa [11–15], we sampled five of the 12 currently recognized species through field surveys. Based on morphology and distribution, these selected taxa are representative across taxonomic sections and exhibit the characteristic East Asian-North American disjunction. With the exception of *C. luteum*, which was sampled from the USA (Alabama), the remaining samples were sourced from East Asia (China, the Republic of Korea, and Japan). These samples were identified using morphological approaches and verified by either co-authors of this study or the corresponding collectors and then deposited in professional institutions or private herbaria. Detailed voucher information regarding the study materials, including sampling location, species appraiser, and specimen source, is presented in Table S2. Silica gel-dried leaves of *Chamaelirium* species were used for sequencing in this study, and high-quality DNA extraction, library preparation, and sequencing were performed by Novogene (Beijing, China). Sequencing libraries were generated using the NEB Next® Ultra DNA Library Prep Kit for Illumina®, and the prepared libraries were sequenced on an Illumina HiSeq 4000 platform according to the manufacturer's recommendations.

Plastid genome assembly, annotation, and comparative analyses

GetOrganelle v1.7.4.1 [52] was used to de novo assemble plastid genomes with reference to the following parameters: -F plant_cp -R 15 -t 8 -k 75, 105, 115, 127. The preliminary assembly results were visualized in Bandage v.8.1 to assess the quality of the assembly [53]. All circular plastid genome sequences were annotated on the web page GeSeq (https://chlorobox.mpimpgolm.mpg.de/geseq.html) [54], and then the annotation results were manually checked and adjusted in Geneious v.9.0.2 [55]

with *Chamaelirium japonicum* (GenBank accession: KF951065) as the reference to correct annotation accuracy. The complete plastid genome map was drawn using OGDRAW (https://chlorobox.mpimp-golm.mpg.de/OGDraw.html) [56]. Plastid genome boundaries were visualized using the IRscope online program (https://irscope.shinyapps.io/irapp/) [57]. The gene selection pressure analysis was performed on the Genepioneer platform (http://cloud.genepioneer.com:9929) with the following settings in calculating the Ka/Ks values: genetic code Table 11 (bacterial and plant plastid code); method: YN [58]. For nucleotide diversity analysis, plastid genome sequences were aligned using MAFFT v.7.308 [59], and then CPStools was used to estimate Pi values [60].

Phylogenetic reconstruction

In order to reconstruct the phylogenetic status of *Chamaelirium*, the phylogenetic matrix integrated five newly sequenced *Chamaelirium* plastomes with 14 genome accessions of other related taxa from the NCBI (National Center for Biotechnology Information, https://www.ncbi.nlm.nih.gov/) (for GenBank accessions, see Table S3). We referred to Kim et al. [16] and Yang et al. [38] to root the tree using *Calochortus* Pursh and *Smilax* L. 82 shared plastid CDS were extracted from each sample for subsequent phylogenetic reconstruction, and sequence alignment was conducted using MAFFT v.7.308 with manual adjustment. Phylogenetic inference was performed based on BI and ML analyses. For BI analysis, GTR + I + G was selected as the best-fitting model according to the Akaike information criterion (AIC) in jModelTest2 v.2.1.6 [61]. The Markov chain Monte Carlo analyses were run with four simultaneous chains of 10,000,000 generations and tree sampling every 1,000 generations. After the first 25% of trees were discarded as burn-in, the remaining trees were used to construct a majority-rule consensus tree with Bayesian posterior probabilities by using MrBayes v3.2.7a [62] on the CIPRES Portal (https://www.phylo.org/). The ML analysis was performed using IQ-TREE v.2.0.3 with 1,000 bootstrap replicates, and the optimal model TVM + F + R2 was selected by Bayesian Information Criteria (BIC) [63].

Species occurrence, climate data, and niche modeling

Occurrence data for five *Chamaelirium* species in the phylogeny were obtained from the Global Biodiversity Information Facility (GBIF, https://www.gbif.org/), field work records, and specimen information from the Chinese Virtual Herbarium (CVH, http://www.cvh.ac.cn/). After manually checking the distribution data to remove duplicates, assumed cultivation records, and other unlikely location coordinates, in order to avoid spatial autocorrelation and sampling bias, only one occurrence of each species was kept in a grid of 10×10 km cells [64]. Finally, a total of 719 occurrences of five species were retained (Table S4), and 19 bioclimatic factors with a spatial resolution of 2.5 arc min for current climatic conditions (1970–2000) were downloaded from WorldClim v.2.1 for subsequent analysis [65]. Climatic niche modeling for each section of *Chamaelirium* was performed using MaxEnt v.3.4.4 [66], setting autofeatures with 10 replicates and 25% locality data as the testing dataset. ENMtools was used to assess correlations between 19 climatic factors, and highly correlated bioclimatic variables were removed (correlation coefficient values of >|0.8|). We kept eight bioclimatic factors for niche modeling: (i) annual mean temperature (bio1), (ii) mean diurnal range (bio2), (iii) isothermality (bio3), (iv) temperature annual range (bio7), (v) precipitation of driest month (bio14), (vi) precipitation seasonality (bio15), (vii) precipitation of warmest quarter (bio18), and (viii) precipitation of coldest quarter (bio19).

Divergence time Estimation and ancestral distribution region reconstruction

Given the absence of reported fossil records for Melanthiaceae and its close relatives, we adopted the dating strategy following Yang et al. [38] according to a previous study [67]. We applied three time points to calibrate the phylogenetic tree: (i) the crown age constraint of 84.8 Ma for Melanthiaceae, (ii) a divergence age of 74 Ma for the split between the Parideae-Xerophyllideae clade and the Chionographideae-Heloniadeae clade, and (iii) the crown age of 52.3 Ma for the divergence between tribes Parideae and Xerophyllideae. These critical age estimates were derived from 17 fossil calibrations across the monocots and major clades of angiosperms [67]. Divergence time estimation was conducted using BEAST v2.4.7 [68], with parameters configured in BEAUti v1.10.4. The GTR + I + Γ substitution model, identified as optimal by jModelTest2 v2.1.6, and the uncorrelated lognormal relaxed clock and the Yule tree prior were selected. Two independent BEAST runs were performed, each comprising 400 million generations, with sampling every 1,000 generations. Convergence of the BEAST analyses was assessed using Tracer v1.5 [69], ensuring that all parameters achieved effective sample sizes (ESS) exceeding 200. The initial 25% of sampled trees were discarded as burn-in, and a maximum clade credibility (MCC) tree was generated in TreeAnnotator v1.10.4.

We reconstructed the ancestral region of *Chamaelirium* using the Bayesian binary MCMC method (BBM) in RASP v4.4 [70]. Considering the lack of taxa representing specific distribution regions in the most recent sister clade of *Chamaelirium*, outgroups were consequently excluded, and two distribution areas, East Asia and North America, were divided and coded in the BBM analysis.

Based on the pruned MCC tree derived from the BEAST analysis, we set ten MCMC chains running simultaneously for 20 million generations, sampling every 1,000 generations and discarding the first 25% of trees as burn-in, under the fixed JC model and the temperature parameter of 0.1.

Supplementary Information

The online version contains supplementary material available at https://doi.org/10.1186/s12870-025-07408-7.

Supplementary Material 1. Supplementary Material: Fig. S1: Adaptive evolutionary analysis for Chamaelirium based on shared protein-coding gene (CDS). Genes marked in red with "*" produce undefined Ka/Ks values (corresponding to the fade-out area). Fig. S2: Nucleotide diversity (Pi) of (A) intergenic regions (IGS) and (B) gene regions (GS) in the Chamaelirium plastome. Highly variable loci in IGS (Pi >0.05) and GS (Pi >0.0125) regions are marked out. Table S1: Genes in the Chamaelirium plastomes are sorted by function. "*" labeled gene with intron and "a" labeled gene duplicated in the IR regions, rps16 is absent in C. japonicum and C. koidzumianum. Table S2: Detailed information on sequencing materials for this study. Table S3: Taxa used for phylogenetic analysis. GenBank accessions marked with "*" were newly generated in this study. Table S4: Distribution coordinates of Chamaelirium species used for niche modeling

Acknowledgements

We are deeply grateful to Zhong-cheng Liu, Lei Wang, and Wen-bo Liao (Sun Yat-sen University) for providing the sequencing materials of Chamaelirium chinense and Chamaelirium viridiflorum for this study. We also extend our sincere appreciation to Wan-yi Zhao (Sun Yat-sen University) and Cheng Zhang (The Orchid Conservation & Research Center of Shenzhen and the National Orchid Conservation Center of China) for offering plant photographs. Special thanks are due to Hoang Dang Khoa Do and Sarah S. Bodin for their professional polishing of the English manuscript.

Authors' contributions

TD, HS and JHK conceived this research and acquired fundings. JYP, XHH and XJZ performed the experiment. JJ and NT offered some research data. JYP, XHH and TD analyzed the data and drafted the manuscript. CK, THK and SYL provided suggestions on structuring the article. All authors have read and agreed to the final manuscript.

Funding

This work was supported under the framework of international cooperation program managed by the National Natural Science Foundation of China (32322006), the Key Projects of the Joint Fund of the National Natural Science Foundation of China (U23A20149), the Second Tibetan Plateau Scientific Expedition and Research (STEP) program (2019QZKK0502), and the National Research Foundation of Korea (NRF-2020K2A9A2A06069516).

Data availability

All newly generated plastid genome data in this study are available in the National Center for Biotechnology Information (https://www.ncbi.nlm.nih.gov/nuccore/), with GenBank accession numbers shown in Table 1.

Declarations

Ethics approval and consent to participate

The authors confirm that appropriate permissions were obtained for plant materials collection, and the sampling was conducted in accordance with local regulations. No materials from animals, humans, or any protected/endangered species were utilized in this study.

Consent for publication

Not applicable.

Competing interests

The authors declare no competing interests.

Author details

[1]State Key Laboratory of Plant Diversity and Specialty Crops, Kunming Institute of Botany, Chinese Academy of Sciences, Kunming 650201, China
[2]Division of Botany, Honam National Institute of Biological Resources, 99, Gohadoan-gil, Mokpo-si 58762, Republic of Korea
[3]Department of Island and Coast Biodiversity, Honam National Institute of Biological Resources, 99, Gohadoan-gil, Mokpo-si 58762, Republic of Korea
[4]Division of Forest Biodiversity, Korea National Arboretum, 509, Gwangneungsumogwon-ro, Pocheon-si 11186, Republic of Korea
[5]Otsuka, Hachioji-shi, Tokyo 192-0352, Japan
[6]Faculty of Health and Life Sciences, INTI International University, Nilai, Negeri Sembilan 71800, Malaysia
[7]Department of Life Sciences, Gachon University, 1342, Seongnam-daero, Seongnam-si 13120, Republic of Korea

Received: 28 June 2025 / Accepted: 11 September 2025
Published online: 06 October 2025

References

1. Raven PH. Plant species disjunctions: A summary. Ann Mo Bot Gard. 1972;59:234–46.
2. Perez-Gutierrez MA, Romero-Garcia AT, Fernandez MC, Blanca G, Salinas-Bonillo MJ, Suarez-Santiago VN. Evolutionary history of fumitories (subfamily fumarioideae, Papaveraceae): An old story shaped by the main geological and climatic events in the Northern Hemisphere. Mol Phylogenet Evol. 2015;88:75–92.
3. Huang XH, Deng T, Chen JT, Fu QS, Zhang XJ, Lin N, et al. Spatial distribution patterns and formation of global spermatophytes. J Integr Plant Biol. 2025;00:1–18.
4. Tiffney BH. Perspectives on the origin of the floristic similarity between Eastern Asia and Eastern North America. J Arnold Arbor. 1985b;66:73–94.
5. Wen J, Ickert-Bond S, Nie ZL, Li R. Timing and modes of evolution of eastern Asian-North American biogeographic disjunctions in seed plants. In Darwin's heritage today: proceedings of the Darwin 200 Beijing international conference. Edited by: Long M, Gu H, Zhou Z. Beijing: Higher Education Press; 2010. pp. 252–269.
6. Wen J. Evolution of Eastern Asian and Eastern North American disjunct distributions in flowering plants. Annu Rev Ecol Syst. 1999;30:421–55.
7. Tiffney BH, Manchester SR. The use of geological and paleontological evidence in evaluating plant phylogeographic hypotheses in the Northern hemisphere tertiary. Int J Plant Sci. 2001;162:S3–17.
8. Wen J, Nie ZL, Ickert-Bond S. Intercontinental disjunctions between Eastern Asia and Western North America in vascular plants highlight the biogeographic importance of the Bering land Bridge from late cretaceous to neogene. J Syst Evol. 2016;54:469–90.
9. Tiffney BH. The eocene North Atlantic land bridge: its importance in tertiary and modern phytogeography of the Northern hemisphere. J Arnold Arbor. 1985a;66:243–73.
10. Deng T, Nie ZL, Drew BT, Volis S, Kim C, Xiang CL, et al. Does the arcto-tertiary biogeographic hypothesis explain the disjunct distribution of Northern hemisphere herbaceous plants? The case of *Meehania* (Lamiaceae). PLoS ONE. 2015;10:e0117171.
11. Tanaka N. A synopsis of the genus *Chamaelirium* (Melanthiaceae) with a new infrageneric classification including *Chionographis*. Taiwania. 2017;62:157–67.
12. Tanaka N. Diversity in fruit and seed characters of *Chamaelirium* and *Chionographis* (Melanthiaceae). Taiwania. 2017;62:67–74.
13. Liu ZC, Feng L, Wang L, Liao WB. *Chamaelirium viridiflorum* (Melanthiaceae), a new species from jiangxi, China. Phytotaxa. 2018;357:126–32.
14. Tong YH, Li YQ, Guo GX, Dai KY, Zeng YJ, He CM. *Chamaelirium shimentaiense* (Melanthiaceae), a new species from guangdong, China. Nord J Bot. 2020;38:e02634.
15. Qin Y, Tan F, Huang YS, Liu Y. *Chamaelirium Jiuwanshanense* (Melanthiaceae), a new dioecious species from guangxi, China. Taiwania. 2023;68:97–100.

16. Kim C, Kim SC, Kim JH. Historical biogeography of melanthiaceae: a case of out-of-North America through the Bering land Bridge. Front Plant Sci. 2019;10:396.
17. Huang R, Xie XN, Chen AM, Li F, Tian EW, Chao Z. The Chloroplast genomes of four *Bupleurum* (Apiaceae) species endemic to Southwestern china, a diversity center of the genus, as well as their evolutionary implications and phylogenetic inferences. BMC Genomics. 2021;22:714.
18. Peng JY, Zhang XS, Zhang DG, Wang Y, Deng T, Huang XH, et al. Newly reported Chloroplast genome of sinosenecio Albonervius Y. Liu & Q. E. Yang and comparative analyses with other sinosenecio species. BMC Genomics. 2022;23:639.
19. Sheng JJ, Yan M, Wang J, Zhao LL, Zhou FS, Hu ZL, et al. The complete Chloroplast genome sequences of five *Miscanthus* species, and comparative analyses with other grass plastomes. Ind Crop Prod. 2021;162:113248.
20. Chen JT, Lidén M, Huang XH, Zhang L, Zhang XJ, Kuang TH, et al. An updated classification for the hyper-diverse genus *Corydalis* (Papaveraceae: Fumarioideae) based on phylogenomic and morphological evidence. J Integr Plant Biol. 2023;65:2138–56.
21. Bodin SS, Kim JS, Kim JH. Complete Chloroplast genome of chionographis Japonica (Willd.) maxim. (Melanthiaceae): comparative genomics and evaluation of universal primers for Liliales. Plant Mol Biol Rep. 2013;31:1407–21.
22. Jansen RK, Wojciechowski MF, Sanniyasi E, Lee SB, Daniell H. Complete plastome sequence of the Chickpea (*Cicer arietinum*) and the phylogenetic distribution of rps12 and ClpP intron losses among legumes (Leguminosae). Mol Phylogenet Evol. 2008;48:1204–17.
23. Dugas DV, Hernandez D, Koenen EJM, Schwarz E, Straub S, Hughes CE, et al. Mimosoid legume plastome evolution: IR expansion, tandem repeat expansions, and accelerated rate of evolution in ClpP. Sci Rep. 2015;5:16958.
24. Wang YH, Wicke S, Wang H, Jin JJ, Chen SY, Zhang SD, et al. Plastome evolution in the early-diverging legume subfamily cercidoideae (Fabaceae). Front Plant Sci. 2018;9:138.
25. Mohanta TK, Mishra AK, Khan A, Hashem A, Abd_Allah EF, Al-Harrasi A. Gene loss and evolution of the plastome. Genes. 2020;11:1133.
26. Yang J, Park S, Gil HY, Pak JH, Kim SC. Characterization and dynamics of intracellular gene transfer in plastid genomes of *Viola* (Violaceae) and order malpighiales. Front Plant Sci. 2021;12:678580.
27. Ai B, Gao Y, Zhang XL, Tao JJ, Kang M, Huang HW. Comparative transcriptome resources of eleven *Primulina* species, a group of 'stone plants' from a biodiversity hot spot. Mol Ecol Resour. 2015;15:619–32.
28. Hurst LD. The ka/ks ratio: diagnosing the form of sequence evolution. Trends Genet. 2002;18:486–7.
29. Kikuchi S, Asakura Y, Imai M, Nakahira Y, Kotani Y, Hashiguchi Y, et al. A *ycf2*-ftsHi heteromeric AAA-ATPase complex is required for Chloroplast protein import. Plant Cell. 2018;30:2677–703.
30. Wu ZH, Liao R, Yang TG, Dong X, Lan DQ, Qin R, et al. Analysis of six Chloroplast genomes provides insight into the evolution of *Chrysosplenium* (Saxifragaceae). BMC Genomics. 2020;21:621.
31. Li EZ, Liu KJ, Deng RY, Gao YW, Liu XY, Dong WP, et al. Insights into the phylogeny and Chloroplast genome evolution of *Eriocaulon* (Eriocaulaceae). BMC Plant Biol. 2023;23:32.
32. Dong WP, Sun JH, Liu YL, Xu C, Wang YH, Suo ZL, et al. Phylogenomic relationships and species identification of the Olive genus *Olea* (Oleaceae). J Syst Evol. 2021;60:1263–80.
33. Li QJ, Liu Y, Wang AH, Chen QF, Wang JM, Peng L, et al. Plastome comparison and phylogenomics of *Fagopyrum* (Polygonaceae): insights into sequence differences between *Fagopyrum* and its related taxa. BMC Plant Biol. 2022;22:339.
34. Kipkoech A, Li K, Milne RI, Oyebanji OO, Wambulwa MC, Fu XG, et al. An integrative approach clarifies species delimitation and biogeographic history of *Debregeasia* (Urticaceae). Plant Divers. 2025;47:229–43.
35. Huang XH, Peng JY, Lin N, Liu J, Chen JT, Liu Q, et al. Climatic niche divergence and long-distance dispersal contributed to the Pantropical intercontinental disjunctions of a liana lineage (*Uncaria*, Rubiaceae). Plant Divers. 2025;47:772–83.
36. Bossert S, Freitas FV, Pauly A, Zhu GP, Crowder DW, Orr MC, et al. Phylogeny, antiquity, and niche occupancy of *Trinomia* (Hymenoptera: Halictidae), an Afrotropical endemic genus of Nomiinae. Mol Phylogenet Evol. 2025;204:108273.
37. Smith BE, Johnston MK, Lücking R. From GenBank to GBIF: phylogeny-based predictive niche modeling tests accuracy of taxonomic identifications in large occurrence data repositories. PLoS ONE. 2016;11:e0151232.
38. Yang LF, Yang ZY, Liu CK, He ZS, Zhang ZR, Yang J, et al. Chloroplast phylogenomic analysis provides insights into the evolution of the largest eukaryotic genome holder, *Paris Japonica* (Melanthiaceae). BMC Plant Biol. 2019;19:293.
39. Yang Y, Chen YS, Zhang JW, Sun L, Sun H. Phylogenetics and historical biogeography of the mock Buckthorn genus (*Sageretia*, Rhamnaceae). Bot J Linn Soc. 2019;189:244–61.
40. Huang XH, Deng T, Chen ST, Landis JB, Lin N, Yang Y, et al. Western Tethys origin, tropical Asia and tropical America Disjunction in berchemia and reinstatement of phyllogeiton (Rhamneae, Rhamnaceae). Taxon. 2021;70:515–25.
41. Deng T, Zhang JW, Meng Y, Volis S, Sun H, Nie ZL. Role of the Qinghai-Tibetan plateau uplift in the Northern hemisphere disjunction: evidence from two herbaceous genera of rubiaceae. Sci Rep. 2017;7:13411.
42. Tiffney BH. Geographic and Climatic influences on the Creta-ceous and tertiary history of Euramerican floristic similarity. Acta Univ Carol Geol. 2000;44:5–16.
43. Nie ZL, Sun H, Beardsley PM, Olmstead RG, Wen J. Evolution of biogeographic Disjunction between Eastern Asia and Eastern North America in *Phryma* (Phrymaceae). Am J Bot. 2006;93:1343–56.
44. Zhou N, Miao K, Liu CK, Jia LB, Hu JJ, Huang YJ, et al. Historical biogeography and evolutionary diversification of *Lilium* (Liliaceae): new insights from plastome phylogenomics. Plant Divers. 2024;46:219–28.
45. Zachos J, Pagani M, Sloan L, Thomas E, Billups K. Trends, rhythms, and aberrations in global climate 65 ma to present. Science. 2001;292:686–93.
46. Li JH, Jiang JH, Vander Stel H, Homkes A, Corajod J, Brown K, et al. Phylogenetics and biogeography of *Apios* (Fabaceae) inferred from sequences of nuclear and plastid genes. Int J Plant Sci. 2014;175:764–80.
47. Sun XJ, Wang PX. How old is the Asian monsoon system?-Palaeobotanical records from China. Palaeogeogr Palaeocl. 2005;222:181–222.
48. Guo ZT, Sun B, Zhang ZS, Peng SZ, Xiao GQ, Ge JY, et al. A major reorganization of Asian climate by the early miocene. Clim Past. 2008;4:153–74.
49. Liang MY, Guo ZT, Kahmann AJ, Oldfield K. Geochemical characteristics of the miocene Eolian deposits in china: their provenance and climate implications. Geochem Geophy Geosy. 2009;10:Q04004.
50. Ji YH, Yang LF, Chase MW, Liu CK, Yang ZY, Yang J, et al. Plastome phylogenomics, biogeography, and clade diversification of *Paris* (Melanthiaceae). BMC Plant Biol. 2019;19:543.
51. An ZS, Kutzbach JE, Prell WL, Porter SC. Evolution of Asian monsoons and phased uplift of the Himalaya–Tibetan plateau since late miocene times. Nature. 2001;411:62–6.
52. Jin JJ, Yu WB, Yang JB, Song Y, dePamphilis CW, Yi TS, et al. GetOrganelle: a fast and versatile toolkit for accurate de Novo assembly of organelle genomes. Genome Biol. 2020;21:241.
53. Wick RR, Schultz MB, Zobel J, Holt KE. Bandage: interactive visualization of de Novo genome assemblies. Bioinformatics. 2015;31:3350–2.
54. Tillich M, Lehwark P, Pellizzer T, Ulbricht-Jones ES, Fischer A, Bock R, et al. GeSeq-versatile and accurate annotation of organelle genomes. Nucleic Acids Res. 2017;45:W6–11.
55. Kearse M, Moir R, Wilson A, Stones-Havas S, Cheung M, Sturrock S, et al. Geneious basic: an integrated and extendable desktop software platform for the organization and analysis of sequence data. Bioinformatics. 2012;28:1647–9.
56. Greiner S, Lehwark P, Bock R. OrganellarGenomeDRAW (OGDRAW) version 1.3.1: expanded toolkit for the graphical visualization of organellar genomes. Nucleic Acids Res. 2019;47:W59–64.
57. Amiryousefi A, Hyvönen J, Poczai P, Hancock J. IRscope: an online program to visualize the junction sites of Chloroplast genomes. Bioinformatics. 2018;34:3030–1.
58. Ivanova Z, Sablok G, Daskalova E, Zahmanova G, Apostolova E, Yahubyan G, et al. Chloroplast genome analysis of resurrection tertiary relict *Haberlea rhodopensis* highlights genes important for desiccation stress response. Front Plant Sci. 2017;8:204.
59. Katoh K, Standley DM. MAFFT multiple sequence alignment software version 7: improvements in performance and usability. Mol Biol Evol. 2013;30:772–80.
60. Huang LJ, Yu HX, Wang Z, Xu WB. CPStools: A package for analyzing Chloroplast genome sequences. iMetaOmics. 2024;1:e25.
61. Posada D. jModelTest: phylogenetic model averaging. Mol Biol Evol. 2008;25:1253–6.
62. Ronquist F, Teslenko M, van der Mark P, Ayres DL, Darling A, Höhna S, et al. MrBayes 3.2: efficient bayesian phylogenetic inference and model choice across a large model space. Syst Biol. 2012;61:539–42.

63. Nguyen LT, Schmidt HA, von Haeseler A, Minh BQ. IQ-TREE: a fast and effective stochastic algorithm for estimating maximum-likelihood phylogenies. Mol Biol Evol. 2015;32:268–74.
64. Aiello-Lammens ME, Boria RA, Radosavljevic A, Vilela B, Anderson RP. SpThin: an R package for Spatial thinning of species occurrence records for use in ecological niche models. Ecography. 2015;38:541–5.
65. Fick SE, Hijmans RJ. WorldClim 2: new 1-km Spatial resolution climate surfaces for global land areas. Int J Climatol. 2017;37:4302–15.
66. Phillips SJ, Dudík M. Modeling of species distributions with maxent: new extensions and a comprehensive evaluation. Ecography. 2008;31:161–75.
67. Givnish TJ, Zuluaga A, Marques I, Lam VKY, Gomez MS, Iles WJD, et al. Phylogenomics and historical biogeography of the monocot order liliales: out of Australia and through Antarctica. Cladistics. 2016;32:581–605.
68. Bouckaert R, Heled J, Kühnert D, Vaughan T, Wu CH, Xie D, et al. Beast 2: a software platform for bayesian evolutionary analysis. PLoS Comput Biol. 2014;10:e1003537.
69. Rambaut A, Drummond AJ, Xie D, Baele G, Suchard MA, Rambaut A, et al. Posterior summarization in bayesian phylogenetics using tracer 1.7. Syst Biol. 2018;67:901–4.
70. Yu Y, Blair C, He XJ. RASP 4: ancestral state reconstruction tool for multiple genes and characters. Mol Biol Evol. 2020;37:604–6.

Publisher's Note

Springer Nature remains neutral with regard to jurisdictional claims in published maps and institutional affiliations.